Acta Cryst. (1995). D**51**, 380–385

Structure of a Monoclonal Anti-ICAM-1 Antibody R6.5 Fab Fragment at 2.8 Å Resolution

BY MAREK J. JEDRZEJAS

Center for Macromolecular Crystallography, Department of Microbiology, University of Alabama at Birmingham, Birmingham, Alabama 35294, *USA*

JOHN MIGLIETTA AND JOHANNA A. GRIFFIN

Boehringer Ingelheim Pharmaceuticals, Inc., PO Box 368, *Ridgefield, Connecticut* 06877, *USA*

AND MING LUO*

Center for Macromolecular Crystallography, Department of Microbiology, University of Alabama at Birmingham, Birmingham, Alabama 35294, *USA*

(*Received* 11 *March* 1994; *accepted* 26 *September* 1994)

Abstract

The specific binding of the monoclonal murine anti-intercellular adhesion molecule-1 (anti-ICAM-1) antibody, R6.5, inhibits the attachment of neutrophils to endothelium and prevents the attachment of major group human rhinovirus (HRV) to ICAM-1. This binding interferes with the host immune system and, as a result, the R6.5 antibody has been developed as a therapeutic anti-inflammatory and perhaps anti-HRV agent. The variable-region amino-acid sequence of R6.5 was determined from the anti-ICAM-1 cDNA. The crystallization conditions of the Fab fragment of R6.5 were established and the three-dimensional structure was determined by X-ray crystallography. The crystal space group is orthorhombic $P2_12_12_1$, a = 40.36, b = 137.76, c = 91.32 Å, and the highest resolution of recorded reflections is 2.7 Å. The molecular-replacement method using known Fab structures was employed to solve the R6.5 Fab structure. The final R factor is 18.8% for a total of 3320 non-H protein atoms, 39 water molecules and 10 606 unique reflections. The protein exhibits the typical immunoglobulin fold. The surface contour of the antigen-combining site of the R6.5 antibody has a wide groove which resembles more the structure of an anti-polypeptide antibody than the structure of an anti-protein antibody.

Introduction

The adhesive interaction between cells and the extracellular matrix and among cells are crucial to developmental processes, immune function, and host defense (Singer, 1990; Springer, 1990; Rothlein, Czajkowski & Kishimoto, 1995). Within the CD18 family of integrin molecules is the leukocyte function associated (LFA-1) protein which is expressed on several cell types including neutrophils and some T-lymphocytes. One of the ligands for LFA-1 is the intercellular adhesion molecule-1 (ICAM-1) which is expressed on endothelial cells and antigen-presenting cells (Kishimoto *et al.*, 1989; Dustin, 1990). The expression of ICAM-1 is induced by cytokines that are produced at sites of inflammation. This serves to enhance neutrophil adherence to endothelial cells and migration from the circulation into extracellular tissues at these sites. Neutrophils contribute further to the inflammatory process by releasing tissue-damaging mediators. Therefore, ICAM-1–LFA-1 interactions are a major step in the inflammation-mediated tissue destruction and graft rejection.

Electron micrographs show that ICAM-1 is shaped like a bent rod, 18.7 nm long and with a diameter of 2–3 μm consisting of five extracellular immunoglobulin-like domains (Staunton, Dustin, Erickson & Springer, 1990). Although the LFA-1 adhesion function has been mapped to the two distal domains 1 and 2 of ICAM-1, terminal domain 1 is responsible for the most important interactions with the LFA-1 (Staunton *et al.*, 1990; Kolatkar *et al.*, 1992). The monoclonal antibody R6.5 binds to a site on domains 1 and 2 blocking the ICAM-1–LFA-1 interaction, thereby preventing the attachment of T-lymphocytes and neutrophils to target cells (Smith *et al.*, 1988; Kolatkar *et al.*, 1992). The R6.5 antibody, by inhibiting ICAM-1–LFA-1 interaction, should inhibit neutrophil migration into extravascular tissue and their contribution to the inflammatory process. Blocking this stage of the inflammatory process should inhibit rejection of transplanted tissue and organs. A phase I clinical study with R6.5 suggests that the inhibition of leukocyte adhesion to the endothelium increased kidney-graft survival (Haung *et al.*, 1993). ICAM-1 has also been identified as the receptor for the major group human rhinovirus (HRV) which causes the common cold (Smith *et al.*, 1988; Greve *et al.*, 1989; Staunton *et al.*, 1989; Marlin *et al.*, 1990). The epitopes of HRV and LFA-1

* Author for correspondence.

partially overlap on ICAM-1. For this reason, the R6.5 antibody can also prevent the binding of HRV to its target host cells (Greve *et al.*, 1989; Staunton *et al.*, 1989; Marlin *et al.*, 1990).

Materials and methods

Sequence and crystallization

The sequence of the constant domain of the R6.5 antibody was derived from Kabat, Wu, Reid-Miller, Perry & Gottesman (1992) based on the isotype of the antibody. The sequence of heavy and light chains in the variable domain was derived from the DNA sequence of the cloned murine anti-ICAM-1 gene (Fig. 1). Complementarity-determining regions (CDRs) are those predicted by homology to sequences compiled by Kabat *et al.* (1992).

Purified R6.5 Fab fragments were provided by Boehringer Ingelheim Pharmaceuticals, Inc., and their preparation followed the standard procedure. The Fab antibody protein was concentrated to $\sim$30 mg ml^{-1} in 10 m*M* Tris buffer, pH 7.5. Trials to search for the correct crystallization conditions were carried out by the hanging-drop vapor-diffusion method (McPherson, 1985) using various percentages of PEG 3350 dissolved in 10 m*M* Tris buffer as precipitant. The drops contained 2.5 µl of protein solution and 2.5 µl of the corresponding reservoir solution. Large crystals of R6.5 Fab were grown after seeding 6% PEG drops with small crystals grown in 10% PEG drops. However, these crystals grew fully in less than 4 h and were very mosaic when they were examined in X-ray diffraction experiments. In order to slow down the crystal growth, the reservoir buffer was switched to 40 m*M* borate, pH 8.5. R6.5 Fab protein apparently solubilized better in borate buffer. Crystals suitable for X-ray diffraction studies were grown by seeding 8% PEG drops with small crystals grown in 13% PEG drops. The maximum length of the crystals was 2.0 mm (Fig. 2) and they grew fully in about 2 days.

Heavy chain variable domain

```
                                  |CDRH1|                    |      CDRH2
QVQLQQSGPE  LVRPGVSVKI  SCKGSGYTFI  DYAIHWVKES  HAKSLEWIGV  ISAYSGDTNY
     |                                          |  CDRH3  |
NQKFKGKATM  TVDKSSNTAY  LELARLTSED  SAIYYCARGG  WLLLSFDYWG  QGTTLTVSS
```

Light chain variable domain

```
                              |  CDRL1        |                      |CDRL2
DVVMTQSPLS  LPVSLGDQAS  ISCRSSQSLV  HSNGNNYLHW  YLQKSGQAPK  LLIYKVSNRF
|                                        |  CDRL3   |
SGVPDRFSGS  GSGTDFTLKI  SRVEAEDLGV  YFCSQSTHVP  LTFGGGTKLE  IK
```

Fig. 1. Amino-acid sequence of variable domain of R6.5 monoclonal antibody. CDRL1, CDRL2, CDRL3, CDRH1, CDRH2 and CDRH3 are complimentarity regions for light- and heavy-chain variable domains 1, 2 and 3.

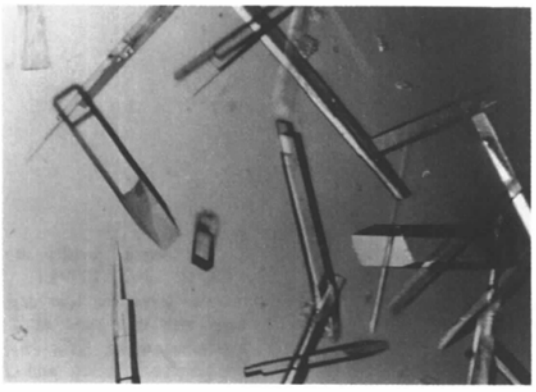

Fig. 2. A photograph of R6.5 Fab crystals grown in a hanging drop. The crystallization conditions are described in *Materials and methods*.

Table 1. *The statistics of the X-ray diffraction data*

Resolution (Å)	No. of observations	No. of unique reflections	% Completion	$I/\sigma(I)$	R_{sym} (%)
4.88	8153	2656	99.5	47.5	5.10
3.87	7024	2501	99.8	35.7	5.50
3.38	5899	2380	96.3	22.2	6.92
3.07	5459	2231	90.7	14.0	9.34
2.85	4271	1900	78.1	7.6	14.43
2.68	1946	930	38.2	4.2	22.1
Totals	32642	12598	84.1	25.2	6.40

Data collection and structure determination

X-ray diffraction data were recorded at room temperature on a Siemens area detector using Cu $K\alpha$ X-rays generated from a Rigaku-200 rotating-anode generator. A single crystal was used to collect 400 frames of data of 0.25° oscillation with an exposure time of 300 s frame^{-1}. The space group is $P2_12_12_1$ with the unit-cell parameters $a = 40.36$, $b = 137.76$, $c = 91.32$ Å, $\alpha = \beta = \gamma = 90°$. The highest resolution of recorded reflections was 2.7 Å. The statistical results of data collection are listed in Table 1.

Coordinates of known Fab structures in the Protein Data Bank at Brookhaven were used to solve the R6.5 Fab structure by the molecular-replacement method. Among the available Fab models, McPC603 produced the best rotation-function peaks and it was ultimately used to solve the structure. The best rotation-function solution using *MERLOT* (Fitzerald, 1988) and diffraction data between 10.0 and 4.0 Å resolution were obtained when the constant (C) domain and variable (V) domain, deleting all six hypervariable regions of McPC603 Fab (Satow, Cohen, Padlan & Davies, 1986), were used separately. Single prominent peaks emerged, with the next peak 80 or 85% of the highest peak for the C and V domains, respectively. The difference in elbow angle between McPC603 and R6.5 was about 37.0°. The orientation of each domain was further refined by the *PC* refinement of *X-PLOR* 3.0 (Brünger, 1990, 1993). The translation was determined by an *R*-factor search using *X-PLOR* and diffraction data between 10.0 and 4.5 Å resolution and the single minimum was found to

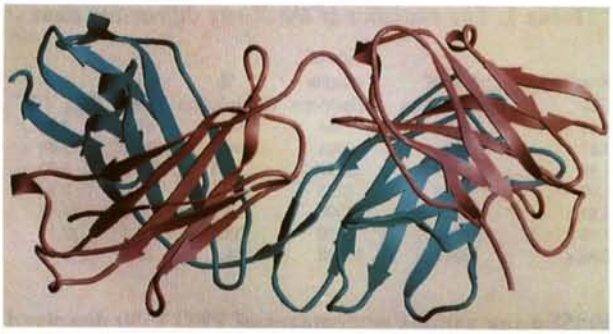

Fig. 3. A ribbon drawing (Carson, 1987) of the R6.5 Fab antibody molecule showing its immunological fold. The heavy chain is depicted in magenta and the light chain is shown in cyan. The constant domain (C_L and C_H1) is on the left; the variable domain is on the right (V_H and V_L) side of the figure.

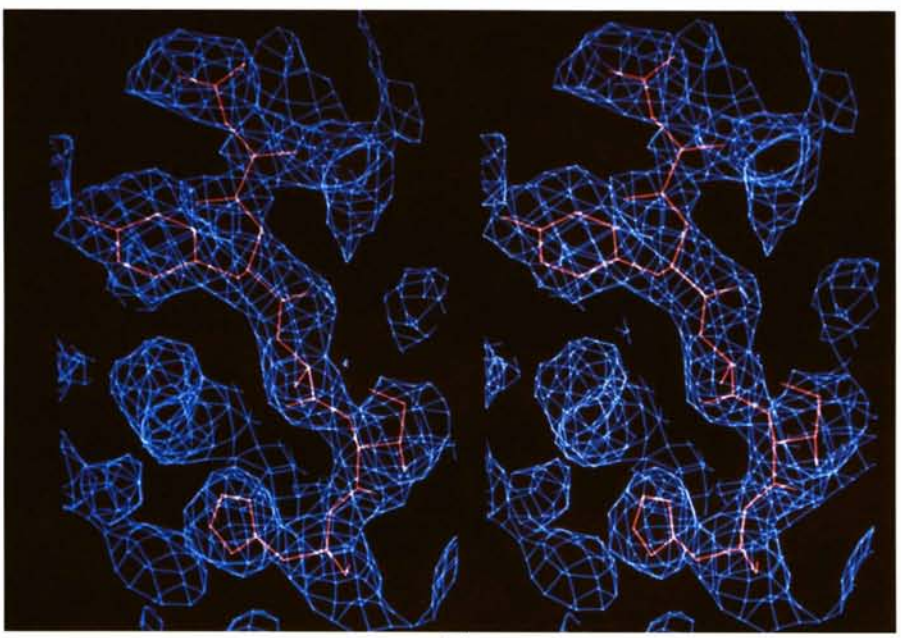

(a)

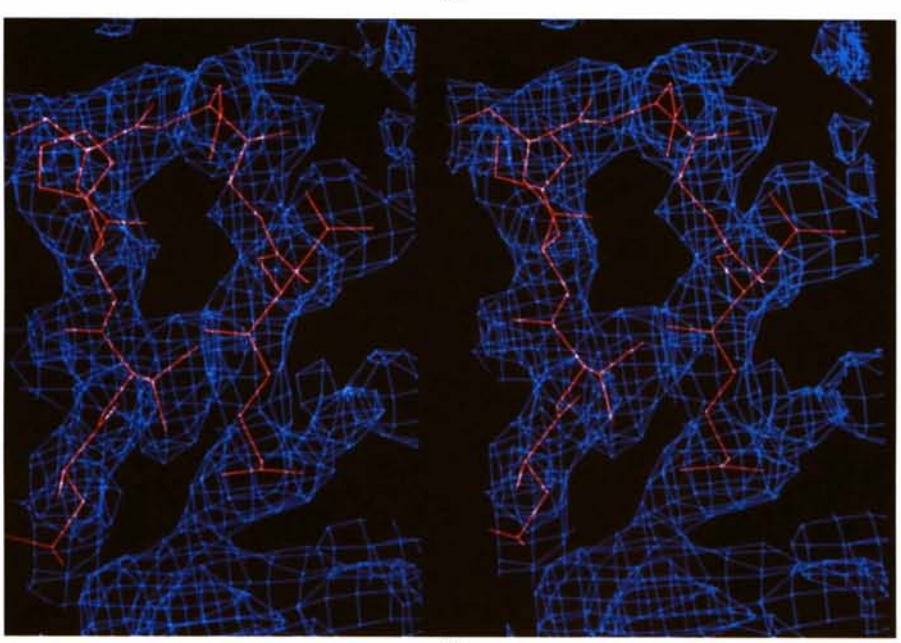

(b)

Fig. 4. Electron density around CDRH1 and CDRL1. The contour level was 1.0σ and the map was calculated at 2.8 Å resolution using $|2F_o - F_c|$ as coefficients. Phases and F_c's were calculated from the final refined coordinates. (*a*) CDRH1, (*b*) CDRL1.

be 50.0%. Molecular packing was acceptable based on visual inspection on an Evans and Sutherland PS300 graphics system utilizing the *FRODO* program (Jones, 1978). Rigid-body refinement treating V_H, V_L, C_H1 and C_L (V_H, V_L, C_H1, C_L = variable or constant domains of heavy or light chains) as individual polypeptide groups yielded R = 37.0%.

Upon rebuilding the model a few insertions and deletions in the sequence relative to McPC603 were taken into account. Subsequent positional least-squares refinement using *X-PLOR* (Brünger, 1993) and diffraction data between 6.5 and 2.8 Å resolution yielded an R factor of 29.0%. $|2F_o - F_c|$ maps at 2.8 Å resolution were calculated by omitting one hypervariable region at a time and the coordinates of each hypervariable region were fitted into its electron-density map on the graphics using the *FRODO* program. Refinement was continued using the simulated-annealing protocol in *X-PLOR* (Brünger, 1993) and the R factor at this stage was 21.1% [$F/\sigma(F) > 4.0$, data 6.5–2.8 Å]. A series of *X-PLOR* simulated-annealing omit maps (Hodel, Kim & Brünger, 1992; Brünger 1993) were also calculated. Few loops were remodeled based on these maps. At the completion of the R6.5 model, the R factor was 18.8%. A total of 3320 non-H protein atoms, 39 ordered water molecules and 10 606 unique reflections [$F/\sigma(F) > 4.0$] between 6.5 and 2.8 Å resolution were used in the refinement. Most of water molecules were located on the protein surface. The averaged r.m.s. values were 0.02 Å from ideal bond lengths, 3.2° from bond angles and 28.2° from dihedral angles. The averaged individual B factor was 16.52 Å^2.

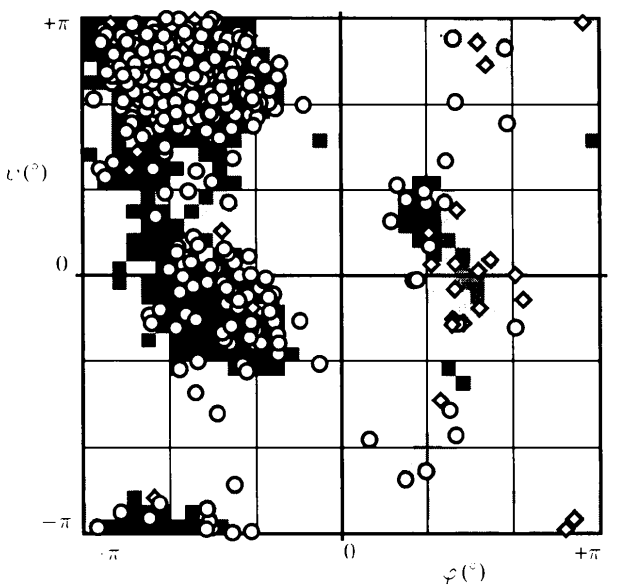

Fig. 5. A Ramachandran plot of ψ and φ angles of 435 residues in the refined R6.5 Fab structure. Circles mark non-glycine residues. Diamonds designate glycine residues. The darkest gray levels represent observed distribution of non-glycine residues. The lightest gray levels represent additional regions for glycine residues. The darker the shading, the more likely the observation. Most of the residues have a β-strand conformation.

Results and discussion

The R6.5 MAb Fab exhibits the typical immunoglobulin fold (Fig. 3). The electron density ($|2F_o - F_c|$ map) is well defined including the area of CDR loops as well as the area of terminal residues. The electron density corresponding to selected CDRs is shown in Fig. 4.

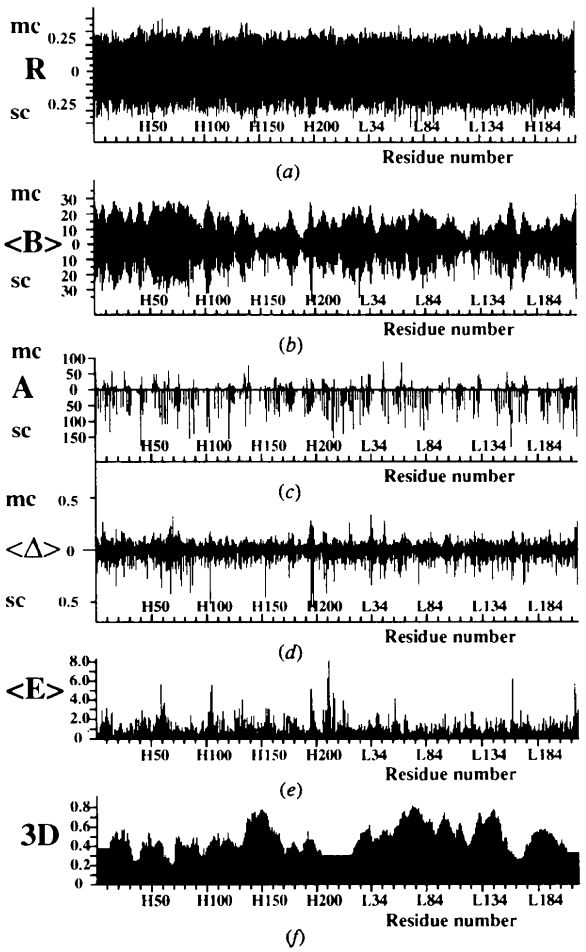

Fig. 6. Evaluation of the quality of the R6.5 Fab final structure based on Brändén & Jones (1990) and Carson *et al.* (1995). (*a*) Real-space electron-density fit per residue, R, computed for main-chain atoms (mc), and for side-chain atoms including Cα (sc). (*b*) Average temperature factor (Å^2) per residue, $\langle B \rangle$, computed for main-chain atoms (mc), and for side-chain atoms including Cα (sc). (*c*) Accessible surface area (Å^2) per residue, A, computed for main-chain atoms (mc), and for side-chain atoms including Cα (sc). (*d*) Coordinate shifts (Å) in the last cycle of simulated-annealing refinement per residue, $\langle \Delta \rangle$, computed for main-chain atoms (mc), and for side-chain atoms including Cα (sc). (*e*) Geometric strain per residue, $\langle E \rangle$, from bond, angle and dihedral energy terms as calculated by *X-PLOR*. (*f*) Three-dimensional profile plot per residue, 3D, smoothed with a 21-residue sliding window.

The geometry of the main-chain atoms is shown in a Ramachandran plot (Fig. 5). This figure shows that with the exception of the terminal residues most residues fall in or near the allowed conformational regions. Some of the Gly residues having positive φ angles are outside of allowed regions. It is, however, not unusual for Gly residues to be found anywhere on the Ramachandran plot. Other residues rarely have conformations that fall outside of allowed regions but such sterically strained conformations do occur in proteins, especially at or near the active site (Herzberg & Moult, 1991). The energy cost that is associated with such a strained conformation is offset by other favorable interactions. The five residues that are significantly outside the allowed regions are located in the loop areas on the surface of the protein and are involved in inter- or intramolecular interactions. The geometry of the side-chain dihedral angles was also examined. As expected, nearly all values lie in the expected regions. An analysis of the structure shows that almost all (81%) of the 435 amino-acid residues with side-chain dihedrals adopt rotamer conformations which fall into conformations described as 'core' conformations (Ponder & Richards, 1987).

A series of charts of different evaluation criteria as suggested by Brändén & Jones (1986) and Carson, Narayana & Bugg (1995) are presented in Fig. 6. Fig. 6(*a*) provides the distribution of the real-space *R* factor (Jones, Zou, Cowan & Kjeldgaard, 1991) that measures the degree of fit of the atomic model to the final map as a function of main-chain and side-chain atoms. The observed temperature factors as a function of residue number for the main- and side-chain atoms are provided in Fig. 6(*b*). The highest *B* factors are in the solvent-exposed loop areas of the structure which indicates their flexibility and/or partial disorder. The lowest *B* factors are located in the β-sheets. The amount of accessible surface area for each residue is plotted in Fig. 6(*c*). As expected, the largest solvent-exposed areas are located in the loop regions. The r.m.s. shift per residue of coordinates between successive runs of simulated-annealing refinement is depicted in Fig. 6(*d*). It has been observed that correctly fitted residues remain essentially in place but flexible or poorly fitted residues deviate from their initial positions. This figure also reveals regions of secondary structure. Geometric strain energy per residue (Brünger, 1993), that can also be associated with problem areas, is shown in Fig. 6(*e*). Fig. 6(*f*) shows the three-dimensional profile plot per residue of R6.5 (Luthy, Bowie & Eisenberg, 1992) based on well refined high-resolution structures. The method has been shown to identify misfolded proteins. The value for correctly folded models averages about 0.4 whereas for incorrectly folded models this value runs typically less than 0.0. Figs. 6(*a*)–6(*f*) all show that the quality of the structure is good.

The R6.5 antigen-combining site

A total of 66 residues are associated with the CDRs and together they represent a solvent-accessible area of 2976 Å^2 (Fig. 7) which accounts for 15.6% of the total accessible area. This is larger than the antigen–antibody contact region (~700 Å^2) observed in other crystal structures of protein antigen–Fab complexes (Amit, Mariuzza, Phillips & Poljak, 1986; Colman *et al.*, 1987; Sheriff *et al.*, 1987; Padlan *et al.*, 1989). Therefore, not all residues of CDR regions are expected to be involved in antigen recognition. Mian, Bradwell & Olson (1991) found that certain amino acids have a higher probability of being located in the antibody-combining site. Tyr, Ser, Trp are the most frequently found whereas Gln, Val, Leu are the least frequently found residues in combining sites. In the CDRs of R6.5 there is only one tryptophan (TrpH101), four tyrosines, and 11 serines. TrpH101 followed by three leucines is located on the flexible CDRH3 loop in the center of the combining site. This may reflect its role in interacting with the antigen. Some

Fig. 7. The surface contour of R6.5 CDRs. The color code for CDRs is, CDRL1, magenta, L2, dark blue, L3, light blue, CDRH1 red, H2, green and H3, yellow. The drawing was made using the *RIBBONS* program (Carson, 1987).

of the serine side chains are also near TrpH101. Charged residues are often involved in specific interactions with antigen. There are two potentially charged residues, HisL31 on CDRL1 and HisL98 on CDRL3, in the central region of the combining site, and they might be involved in specific charge interactions with acidic residues on the antigen.

In several cases, protein antigen–antibody interaction is *via* a somewhat flat surface (Amit *et al.*, 1986; Colman *et al.*, 1987; Sherif *et al.*, 1987; Padlan *et al.*,1989). However, some peptide–antibody complexes seem to show that the antigen fits into a groove in the antibody-combining site (Rini, Schulze-Gahmen & Wilson, 1992). R6.5 may resemble the peptide–antibody interaction since it has a similar CDR structure as that of McPC603 which binds to a small hapten. The presence of a deep groove in the antibody-binding region between CDRH2 and CDRL3 suggests that the ICAM-1 molecule domains D1 or D2 could partially fit there. Some shape changes as well as local tertiary structure alteration may occur with binding.*

We thank Danrey W. Toth for technical assistance in setting up crystallization boxes. The work is supported by a grant from Boehringer Ingelheim Pharmaceuticals, Inc.

* Atomic coordinates and structure factors have been deposited with the Protein Data Bank, Brookhaven National Laboratory (Reference: 1RMF, R1RMFSF). Free copies may be obtained through The Managing Editor, International Union of Crystallography, 5 Abbey Square, Chester CH1 2HU, England (Reference: GR0377).

References

AMIT, A. G., MARIUZZA, R. A., PHILLIPS, C. & POLJAK, R. J. (1986). *Science*, **233**, 717–753.

BRÄNDÉN, C. & JONES, T. A. (1990). *Nature (London)*, **343**, 687–689.

BRÜNGER, A. T. (1990). *Acta Cryst.* A**46**, 46–57.

BRÜNGER, A. T. (1993). *X-PLOR, Version* 3.0 *Manual*, Yale Univ., New Haven, CT, USA.

CARSON, M. (1987). *J. Mol. Graphics*, **5**, 103–106.

CARSON, M., NARAYANA, S. V. L. & BUGG, C. E. (1995). *Acta Cryst.* D**51**. In preparation.

COLMAN, P. M., LAVER, W. G., VARGHESE, J. N., BAKER, A. T., TULLOCH, P. A., AIR, G. M. & WEBSTER, R. G. (1987). *Nature (London)*, **326**, 358–363.

DUSTIN, L. D. (1990). *BioEssays*, **12**, 421–427.

FITZERALD, P. M. D. (1988). *J. Appl. Cryst.* **21**, 273–278.

GREVE, J. M., DAVIS, G., MEYER, A. M., FORTE, C. P., YOST, S. C., MARLOR, C. W., KAMARCK, M. E. & MCCLELLAND, A. (1989). *Cell*, **56**, 839–847.

HAUNG, C. E., COLVIN, R. B., DELMONICO, F. L., AUCHINOCLOS, H., TOLKOFF-RUBIN, N., PREFFER, F. I., RPTHLEIN, R., NORRIS, S., SCHARSCHMIDT, L. & COSIMI, A. B. (1993). *Transplantation*, **55**, 766–773.

HERZBERG, O. & MOULT, J. (1991). *Proteins Struct. Funct. Genet.* **11**, 223–229.

HODEL, A., KIM, S. H. & BRÜNGER, A. T. (1992). *Acta Cryst.* A**48**, 851–858.

JONES, T. A. (1978). *J. Appl. Cryst.* **11**, 268–272.

JONES, T. A., ZOU, J.-Y., COWAN, S. W. & KJELDGAARD, M. (1991). *Acta Cryst.* A**47**, 110–119.

KABAT, E. A., WU, T. T., REID-MILLER, M., PERRY, H. M. & GOTTESMAN, K. S. (1992). *Sequences of Proteins of Immunological Interest.* Betheseda, MD, USA: National Institutes of Health.

KISHIMOTO, T. K., LARSON, R. S., COBRI, A. L., DUSTIN, M. L., STAUNTON, D. E. & SPRINGER, T. A. (1989). *Adv. Immunol.* **46**, 149–182.

KOLATKAR, P. R., OLIVEIRA, M. A., ROSSMANN, M. G., ROBBINS, A. H., KATTI, S. K., HOOVER-LITTY, H., FORTE, C., GREVE, J. M., MCCLELLAND, A. & OLSON, N. H. (1992). *J. Mol. Biol.* **225**, 1127–1130.

LUTHY, R., BOWIE, J. U. & EISENBERG, D. (1992). *Nature (London)*, **356**, 83–85.

MARLIN, S. D., STAUNTON, D. E., SPRINGER, T. A., STRATOWA, C., SOMMERGRUBER, W. & MERLUZZI, V. J. (1990). *Nature (London)*, **344**, 70–72.

MCPHERSON, A. (1985). *Methods Enzymol.* **114**, 112–120.

MIAN, S., BRADWELL, A. R. & OLSON, A. J. (1991). *J. Mol. Biol.* **217**, 133–151.

PADLAN, E. A., SILVERTON, E. W., SHERIFF, S., COHEN, E. H., SMITH-GILL, S. J. & DAVIES, D. R. (1989). *Proc. Natl Acad. Sci. USA*, **86**, 5938–5942.

PONDER, J. W. & RICHARDS, J. (1987). *J. Mol. Biol.* **193**, 775–791.

RINI, J. M., SCHULZE-GAHMEN, U. & WILSON, I. A. (1992). *Science*, **255**, 959–965.

ROTHLEIN, R., CZAJKOWSKI, M. & KISHIMOTO, T. (1995). *Chem. Immunol.* In the press.

SATOW, Y., COHEN, G. H., PADLAN, E. A. & DAVIES, D. R. (1986). *J. Mol. Biol.* **190**, 593–604.

SHERIFF, S., SILVERTON, E. W., PADLAN, E. A., COHEN, G. H., SMITH-GILL, S. J., FINZEL, B. C. & DAVIES, D. R. (1987). *Proc. Natl Acad. Sci. USA*, **84**, 8075–8079.

SINGER, K. H. (1990). *J. Leuk. Biol.* **48**, 367–374.

SMITH, C. W., ROTHLEIN, R., HUGHES, B. J., MARICALCO, M. M., SCHMALSTIEG, F. C. & ANDERSON, D. C. (1988). *J. Clin. Invest.* **82**, 746–1756.

SPRINGER, T. A. (1990). *Nature (London)*, **346**, 425–434.

STAUNTON, D. E., MERLUZZI, V. J., ROTHLEIN, R., BARTON, R., MARLIN, S. D. & SPRINGER, T. A. (1989). *Cell*, **56**, 849–853.

STAUNTON, D. E., DUSTIN, M. L., ERICKSON, H. P. & SPRINGER, T. A. (1990). *Cell*, **61**, 243–254.